Proceedings of the 2000 IEEE
International Conference on Robotics & Automation
San Francisco, CA • April 2000

Instantaneous Evaluation of Friction Based on ARTC Tactile Sensor

Hiroyuki SHINODA, Shinya SASAKI, and Katsuhiko NAKAMURA

Department of Electrical & Electronic Engineering,
Tokyo University of Agriculture & Technology
2-24-16 Koganei, Tokyo 184-8588 Japan
shino@cc.tuat.ac.jp

Abstract

A human can lift up an object with almost minimal grasping force regardless of the friction coefficient between the fingers and the object, but the sensing mechanism for this remarkable task has not been well explicated yet. In this paper we propose a tactile sensor to detect a friction coefficient at the moment of touch. With this sensor output we evaluate the largest lifting-force just before a slip happens, without any preliminary motions. The sensor has a sensing cell in the elastic body, which measures strain/stress components parallel and vertical to the surface. Those plural stress/strain parameters at a point gives the friction coefficient. A prototype sensor is fabricated with acoustic resonant tensor cell, and we examine that principle in experiments.

Key words: *tactile sensor, grasping, acoustic resonant tensor cell*

1 Introduction

A human can lift up an object with almost minimal grasping force regardless of the friction coefficient between the fingers and the object [1], but the sensing mechanism for this remarkable task has not been well explicated yet. One strategy to mimic this task in robotics is pre-perception of the friction coefficient by rubbing an object with the finger before grasping. However it needs not only some preliminary motions unlike a human, but also needs sophisticated finger control for the sensing.. In other approaches, some friction-detectable tactile sensors have been proposed, which detect dynamic signals [2] or slight changes of shearing stress distribution [3] occurring at the slip outset. But the dynamic signal happening sporadically is not easy to use in a practical system. In this paper we pay attention to a stress component, 'tangential stress' (See **Fig. 1**) in the sensor skin, which had not drawn technological attention in tactile sensor design. We present a sensor which detects both normal and tangential strain/stress simultaneously, can detect the frictional coefficient between the sensor and the object. The detection is stable, and it is done instantaneously, at the outset of touching. The elastic sensing cell is easily realized by ARTC tactile sensor [4]. Using this sensor we will easily realize the "minimal force grasping" simply by gradually increasing both the gripe force and lift force according to the sensor signal.

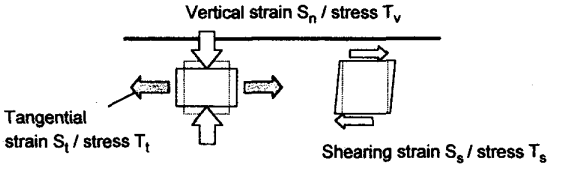

Fig. 1: The terminology of strain component in this paper. We call normal strain/stress component along the surface "Tangential strain/stress," while we simply call normal strain/stress vertical to the surface "Vertical strain/stress."

2 Basic principle

Suppose a tactile sensor has a sensing element to detect both vertical and tangential strain. See **Fig. 1**. When a rigid object is pressed on the sensor as shown in **Fig. 2**,

the vertical stress distribution $T_v(x)$ at the surface is half-elliptical under the Hertz condition. Here we consider two extreme cases.

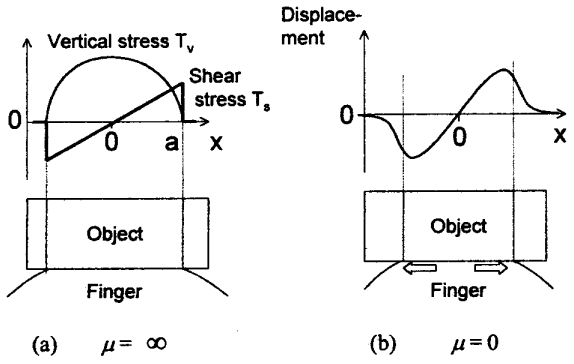

Fig. 2: (a) When the friction is large, the sensor skin surface does not move horizontally, and shear stress arises. (b) For frictionless object, the finger skin extends horizontally. In this illustration, we give positive value to compressive stress.

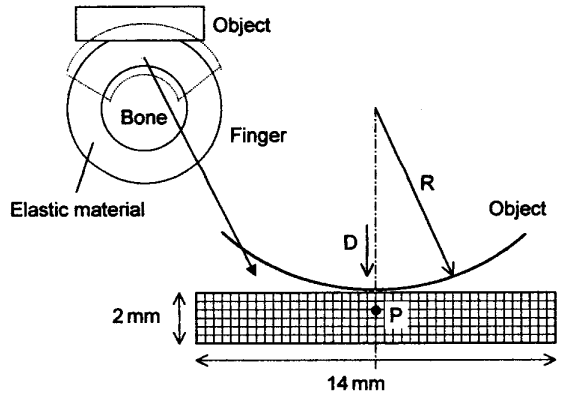

Fig. 3: The elastic body for 2-D FEM analysis. For convenience of calculation, we developed the rounded skin into a plane elastic body. The bottom is fixed only vertically, and can move horizontally. Poisson ratio of the material is 0.48. The 2-D analysis in this paper is equivalent to a 3-D analysis constraining perpendicular displacement to this sheet to be zero.

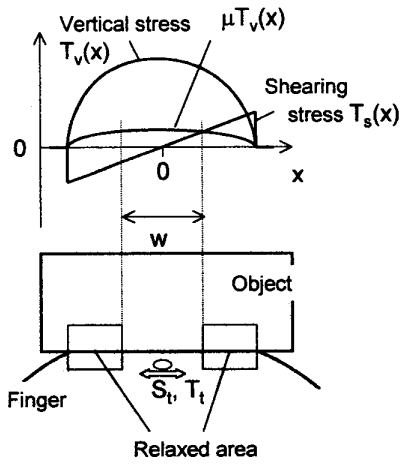

Fig. 4: The curve of $T_s(x)$ is the theoretical shearing stress for $\mu = \infty$. Out of the area W, where $T_s > \mu T_v$, a slip should happen. The sensor detects both vertical and tangential strain under the surface.

Case 1: The friction coefficient is zero, then sensor skin extends horizontally, and small slips arise overall the contact area.

Case 2: The friction coefficient is sufficiently large, then the skin can not move horizontally, and a shearing stress distribution $T_s(x)$ arises as shown in **Fig. 2** (a). The illustration of the $T_s(x)$ is based on the results of FEM analysis for a developed plane elastic body as shown in **Fig. 3**. Regardless of the radius R and D, the $T_s(x)$ is qualitatively given as

$$T_s(x/a) \begin{cases} \approx 0.4\dfrac{x}{a}T_n(0) & [|x|<a] \\ = 0 & [|x|>a] \end{cases}, \qquad (1)$$

where $2a$ is the width of the contact area.

Thus, the way of horizontal extension of the sensor skin depends on the friction between the sensor skin and the object.

As a next step, consider an imaginary experiment, in which the friction coefficient changed abruptly from infinitely large value to a finite value μ. Then slip would happen outside of the area W where a condition $T_s(x) < \mu T_v(x)$ is satisfied, and the width of W depends on the friction coefficient μ. See **Fig. 4** and **Fig. 5**. When μ is smaller than 1, we can expect the width W influences the tangential stress under the contact.

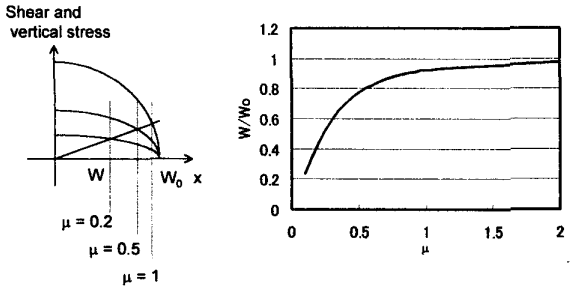

Fig. 5: The width of W in **Fig. 4** versus friction coefficient.

3 Results of FEM analysis

Next we calculate deformation of the elastic body in frictional contact by 2-D FEM. Though actual contact phenomenon involving slip is complex, we obtain qualitative properties in an approximation [3].

As **Fig. 3** shows, a cylinder with radius R is gradually pressed down to the final displacement D. We divide this transition into N, and evaluate the surface movement for each displacement D/N as follows.

<0> Assume the cylinder is placed so that its bottom is D/N below the sensor surface.

<1> Give vertical displacement (without lateral movement) to each nodal point which corresponds to surface of elastic body so that the nodal point yields to the cylinder shape.

<2> Search points P_1 s receiving upward force. If no P_1 exists, jump to <4>.

<3> Calculate the deformation without displacement constraint on P_1 s, and return to <2>.

<4> Search points P_2 s which have larger tangential force than the maximal static friction, and recalculate the FEM without lateral displacement constraint on P_2 s. (Fix only vertical displacement.)

<5> Put the cylinder down by D/N, and return to <1>.

Fig. 6 shows the results of S_v (vertical strain) and T_t (tangential stress) for μ at a point P, the center of the contact and 0.7 mm under the surface. The stress plots show stress divided by Young's modulus T_t/E. As **Fig. 3** shows, the thickness and width of elastic body are 2 mm and 14 mm, respectively. The radius of the object cylinder is 2.4 cm. The mesh size for FEM calculation is uniformly 0.2 mm square. In the following analysis, we only fix the bottom of the elastic body vertically, that is, we allow free lateral movement at the bottom. Each step of object movement D/N was 2 μm. We selected the value of N seeing the convergence of the results.

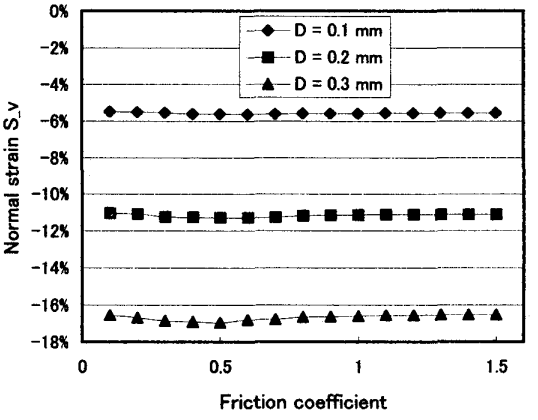

(a)

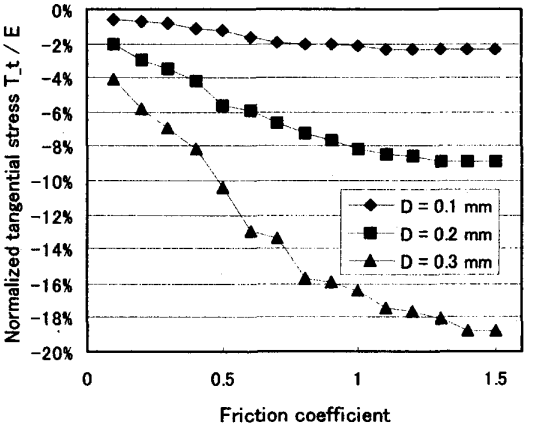

(b)

Fig. 6: FEM results of (a): vertical strain S_v and (b): tangential stress T_t for μ at the point P, the center of the contact and 0.7 mm under the surface.

As **Fig. 6** (a) shows, the vertical strain S_{nv} does not depend on the friction coefficient μ. On the other hand, the tangential stress T_n changes obviously by μ. Therefore this physical parameter should be used for friction sensing, though the curve is also influenced by pressing depth D and curvature of sensor/object R.

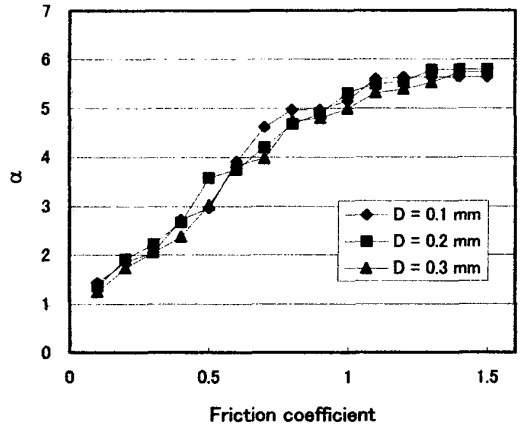

Fig. 7: Plots of $\alpha = T_t/(E|S_v|^{1.9})$ for pressing depth D = 0.1 mm, 0.2 mm, and 0.3 mm. The three curves overlap, which means the α can be an indicator for μ.

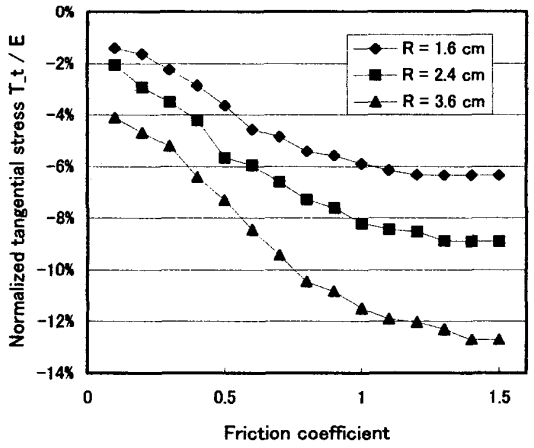

Fig. 8: Plots of tangential stress T_t for object radius R = 1.6, 2.4, and 3.6 cm. Pressing depth D is 0.2 mm.

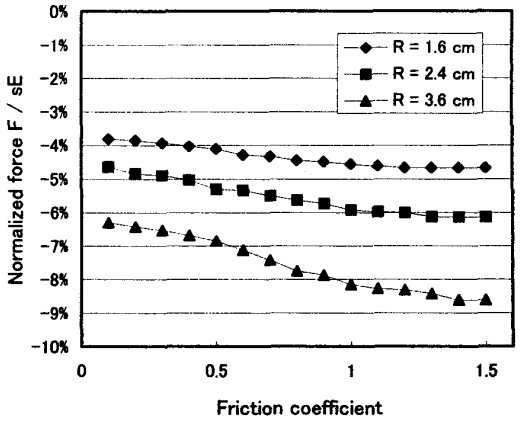

Fig. 9: Plots of total pressing force F received by the sensor for object radius R = 1.6, 2.4, and 3.6 cm. Pressing depth D is 0.2 mm. The E and s are Young's modulus and the sensor area, respectively.

4 Friction sensing

The following two a-priori-conditions

1) the object is sufficiently harder than the sensor, and
2) the curvature of the object is sufficiently smaller than the sensor curvature

will not strongly limit this sensor's application area. If the R is constant, only two parameters μ and D determine the stress at P. As we saw in **Fig. 6** (a), the vertical strain S_v hardly depends on μ, and it is proportional to D. On the other hand, the tangential stress T_t changes largely by μ, for each D. Therefore these two parameters S_v and T_t include sufficient information to determine μ.

Fortunately, there is an easy inversion process to obtain μ. For example, **Fig. 7** shows the plots of the following quantity,

$$\alpha = -\frac{1}{E}\cdot\frac{T_t}{|S_v|^{1.9}} \tag{3}$$

where E is Young's modulus. The three curves for D = 0.1 mm, 0.2 mm, and 0.3 mm are almost overlapped. Thus, the α can be a proper indicator for μ regardless the

pressing depth D, if it is smaller than 1. It is important to note that the α is not influenced by the applied shearing force as long as the point P is at the center of the contact.

Next we discuss sensing various curvature of object. As **Fig. 8** shows, tangential stress depends on the radius R. In general, it is impossible to resolve three parameters μ, D, and R from two degree of freedom of vertical/tangential stress at one observation point P. But if the finger has a macroscopic sensor to get the total force F, it becomes possible theoretically. As we saw in **Fig. 6** (a), the S_v is almost proportional to D regardless of the object radius R. The numerical simulation told that the S_v was constant regardless of R in range from 1.6 cm to 3.6 cm within 2% error for all μs from 0.1 to 1.5. Therefore we can estimate D from S_v easily. For a certain D, it is obvious that the mapping from (μ, R) to (T_t, F) is one to one. As **Fig. 9** shows, the total pressing force F is also changed by the R, but it is less affected by μ than T_t is.

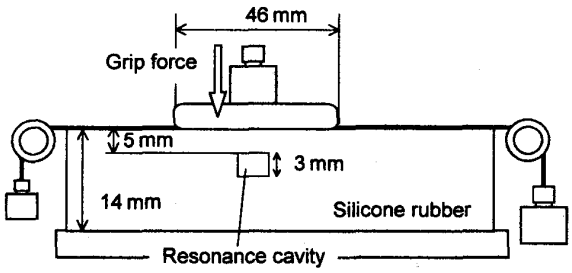

Fig. 10: Experimental setup using ARTC [4,5] tactile device.

5 Sensor fabrication and experimental results

We fabricated an experimental device with plane top surface as shown in **Fig. 10**, using Acoustic Resonant Tensor Cell [4,5] which can detect the extension of the parallelepiped cavity along each side. We observed the cavity extension when we pressed two kinds of objects whose friction coefficients were different. In this experiment, we made both the object and the sensor plane, for convenience. Besides, we fixed the bottom of the elastic body on a rigid plate. Therefore we must note the contact condition is different from the previous analysis.

One object had a clean acrylic surface, and the other had a talcum-powdered surface of the same size and material.

Fig. 11 shows the experimental data of friction coefficient between the sensor and the objects versus normal (grip) force. For clean surface, the μ was ranged between 1.7 and 4.7, while about 0.2 for the powdered one.

Fig. 12 shows the cavity deformation versus normal force. Both the tangential strain and isometric strain (the sum of the three strain components along the three sides) are plotted. Here the "strain" means the cavity's extension. The isometric strain is almost independent of the μ, while the tangential strain shows significant difference in **Fig. 13** which shows the tangential strains of **Fig. 12** in a magnified vertical axis. Here we obtained a sensing parameter to indicate the friction coefficient at the moment of touching.

It is interesting the experimental results in the literature [1] which demonstrates the remarkable ability of the minimum-force-lifting of a human were all for smaller friction coefficients than 1. And it is said Ruffini ending is sensitive to the tangential strain.

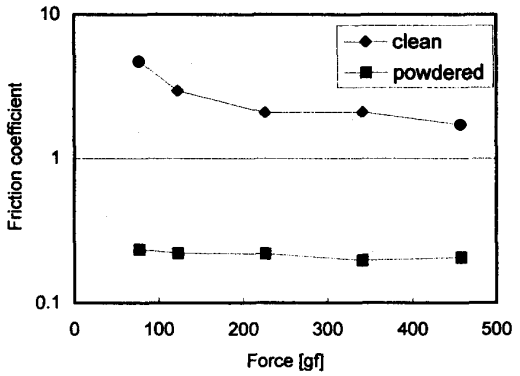

Fig. 11: Friction coefficients of the two samples. A clean acrylic surface and talcum-powdered surface of the same size and material.

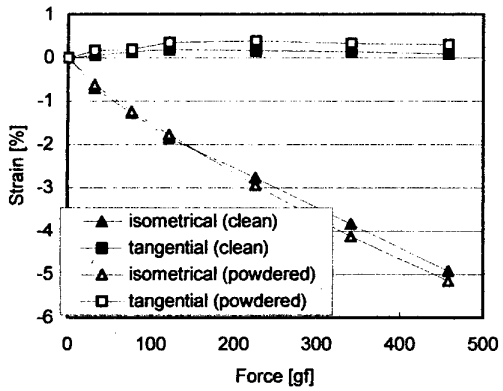

Fig. 12: Measured strains (extensions) of the resonant cavity.

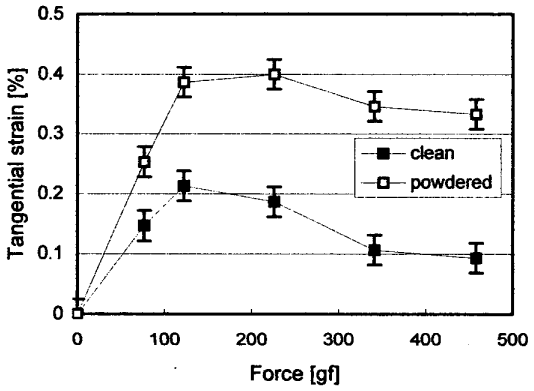

Fig. 13: Measured tangential strains of the resonant cavity. (In a magnified vertical axis.)

6 Summary

In this paper we proposed a principle to sense friction at the moment of touch. With this sensor output we evaluate the largest lifting-force just before a slip happens, without any preliminary motions.

1. Tangential stress under a contact surface is largely changed by the friction coefficient.
2. If the following a-priori-conditions;
   1) the object is sufficiently harder than the sensor, and
   2) the curvature of the object is sufficiently smaller than the sensor curvature,

   are satisfied, the friction coefficient μ (< 1) is evaluated from vertical strain and tangential stress at a certain point under the center of the contact, without other sensor signals.
4. By combining total contact force signal with stress/strain signal, we can sense μ and object's curvature simultaneously.
3. The sensor signal is not influenced by the applied shearing force if the observation point is at the center of the contact.

A prototype sensor was fabricated, and we confirmed the tangential strain of ARTC cavity was changed by the friction.

References

[1] R.S. Johansson and G. Westling, "Roles of Glabrous Skin Receptors and Sensorimotor Memory in Automatic Control of Precision Grip when Lifting Rougher or More Slippery Objects," Exp. Brain Res., 56, pp.550-564, 1984.

[2] M. R. Tremblay and M. R. Cutkosky, "Estimating Friction Using Incipient Slip Sensing During a Manipulation Task," Proc. 1993 IEEE Int. Conf. on Robotics & Automation, pp. 429-434, 1993.

[3] T. Maeno, K. Kobayashi and N. Yamazaki, "Sensing Mechanisms of the Partial Incipient Slip at the Surface of Cylindrical Fingers During the Precision Grip," Proc. ASME Bioengineering Conference, BED-Vol. 35, pp. 117-118, 1997.

[4] H. Shinoda, K. Matsumoto and S. Ando, "Acoustic Resonant Tensor Cell for Tactile Sensing," Proc. 1997 IEEE Int. Conf. on Robotics & Automation, pp. 3087-3092, 1997.

[5] K. Matsumoto, H. Sugimoto, M. Hakozaki, T. Nakajima and H. Shinoda, "Tactile Sensing Element Using Multimode Acoustic Resonance," Proc. IEEJ 15th Sensor Symposium, pp. 95-98, 1997.